



THE 22ND CHESAPEAKE SAILING YACHT SYMPOSIUM

ANNAPOLIS, MARYLAND, MARCH 2016

The influence of sailor position and motion on the performance prediction of racing dinghies

Joshua C Taylor, Performance Sport Engineering Lab, University of Southampton, UK

Joseph Banks, Performance Sport Engineering Lab, University of Southampton, UK

Stephen R Turnock, Performance Sport Engineering Lab, University of Southampton, UK

ABSTRACT

The time-varying influence of a sailor's position is typically neglected in dinghy velocity prediction programs (VPPs). When applied to the assessment of dinghy race performance, the position and motions of the crew become significant but are practically hard to measure as they interact with the motions of the sailboat. As an initial stage in developing a time accurate dinghy VPP this work develops an on-water system capable of measuring the applied hiking moment due to the sailor's pose and compares this with the resultant dinghy motion. The sailor's kinematics are captured using a network of inertial motion sensors (IMS) synchronised to a video camera and dinghy motion sensor. The hiking moment is evaluated using a 'stick man' body representation with the mass and inertial terms associated with the main body segments appropriately scaled for the representative sailor. The accuracy of the pose captured is validated using laboratory based pose measurements. The completed work will provide a platform to model how sailor generated forces interact with the sailboat to affect boat speed. This will be used alongside realistic modelling of the wind and wave loadings to extend an existing time-domain dynamic velocity prediction program (DVPP). The results are demonstrated using a single handed Laser and demonstrate an acceptable level of accuracy.

NOTATION

ν	Kinematic viscosity (N s m^{-2})
ρ	Density of water (kg m^{-3})
P	Pressure (N m^{-2})
LOA	Length over all (m)
BWL	Beam waterline (m)
SA	Sail Area (m^2)
Δ	Total mass displacement (kg)
VPP	Velocity Prediction Programme
L^{seg}	Body segment length (m)
C_g	Segmental centre of gravity (m)
IMU	Inertial Measurement Unit

RMS	Root mean squared
λ	Relative segment centre of gravity
μ	IMU position
a_{IMU}	Acceleration in IMU axis
a_{SEG}	Acceleration in segment axis
m_i	Mass of segment i (kg)

(Tensor, \bar{T} , and vector \vec{T} notation, quaternions are 1x4 vectors which are identified by a bold capital Q)

INTRODUCTION

The rapid rise in the competitive use of foiling yachts either in classes such as the International Moth, the America's Cup or in ocean races requires an ever deeper understanding of the physics of yacht performance. At the smaller scale the behaviour of the sailor, where and how they move, can have a marked effect on overall boat performance. Understanding how the influence of the sailor can be captured during the evaluation of alternative hull-foil design combinations and for overall race prediction analysis motivates the work described.

The performance of sailing boats is commonly assessed by the time required for them to complete a mile-long racecourse. This is calculated using a velocity prediction programme (VPP). The resultant race time is derived by balancing the resistive and propulsive forces acting on the vessel at different points of sail to determine the maximum velocity made good (VMG) around the course. For this method to accurately predict course times sophisticated force modelling is required. This must include the predominant sail and hydrodynamic forces but also the effect of perturbations caused by the naturally varying wind and wave environment as well as the motions of the sailor.

Typically, VPP's assume that the forces are varying in a quasi-steady manner and that the sailor remains in a fixed position to generate a hiking moment. A logical step to assess the significance of this is to extend the VPP to include realistic loadings including the effects of sailors'

motions. To achieve this it is important to understand what the sailor's motions are whilst out sailing and how these effect the righting moment that they are generating. Therefore, this research focuses on the development of a system that is able to estimate the on-water sailor loadings by measuring the dynamic pose of the athlete. The paper layout looks first at the background to dynamics velocity prediction programs (DVPP's) followed by the development of a motion capture system suitable for on-water measurements.

BACKGROUND

Single handed dinghies provide convenient platforms to study the significance of sailor motions. Sailors' essentially have three controls to react to their environment: (1.) Changing course; (2.) Trimming the sail; or (3.) Altering the loading they exert on the boat. The most significant of these loadings is the hiking moment. A change in loading can be in response to a varying wind vector, wave loadings or tactical decisions to events in the race.

A typical response to a long duration wind increase would be to increase the hiking moment by leaning out further. However short duration responses to waves or gusts can be made using rapid body motions which can spill wind from the leech or ease the hull through a wave by controlling trim. Although it is standard practice for the sailor to constantly adapt their hiking moment most VPPs, including unsteady versions, assume the hiking moment to be either constant or simply equal to the wind heeling moment. The current paper presents a technique to capture sailor-induced loadings exerted on the boat using an array of inertial sensors.

Dynamic sailor motions are most significant in tacking and gybing manoeuvres. The tack and gybe manoeuvres have been modelled in detail for yachts (Masayuma et al, 1995; Breschan et al, 2013; Spenkuch et al, 2010; Keuning et al, 2005; De Ridder et al, 2004) but so far has been neglected for dinghies.

The sailor can affect the forces acting on the boat by adjusting the rudder, mainsail and their own position in the boat. Human tactical models based on either rules or decision algorithms have been developed for yacht VPP's (Spenkuch, 2014). While these still assume constant sailor loadings, they have also been extended to include wave induced motions (Keuning, 2005). Spenkuch and Scarponi

(2010) developed the tacking simulations of Matsuyama (1995) to investigate how the effect of human decision making impacts on course time. A Bayesian belief-based human decision engine was developed to include the effects of tactics in a sailing race (Spenkuch, 2011).

Although dynamic body motions are acknowledged in sailing literature to react to short term changes in wind speed and to promote foiling (Findlay and Turnock, 2008), no VPPs or studies into the sailors motions have yet been published. This is despite international sailing rules being developed to prevent sailors from over using such methods (ISAF, 2013).

FULL SCALE ANALYSIS OF MOTIONS INCLUDING DYNAMIC POSE CAPTURE

It is challenging to directly measure a sailor's loading whilst on the water. This is due to the generated hiking moment being transmitted to the hull through a combination of the deck, toe-straps and the mainsheet. Therefore, a method based on wireless inertial sensors is presented to estimate the athlete loadings exerted on the boat. Alternative approaches to capturing motion can include automated video capture. Phillips et al (2014) compared the use of inertial sensors and video motion capture for a swimmers underwater fly-kick and demonstrated comparable accuracy. The advantage of sensors is that they do not rely on high quality images at all times. Disadvantages of using the inertial sensors are associated with sensor drift and ensuring they are operating all the time. For a multi-sensor system the latest sensors are now much more reliable, which offers the opportunity to capture on-water motions as long as issues with waterproofing can be addressed. Similar challenges have been overcome for use in capturing model ship motions (Bennett et al, 2014).

The method we adopt to control the influence of drift is to use our knowledge of the fixed geometry of the sailor. From this the sailor's motion is based on using a kinematic chain. This deliberate simplification allows the model to be calibrated to match the subject's own body segment weights using an anthropometric model as a starting point. This allows subject specific loadings which are required to reverse engineer the sailor's dynamic pose. Figure 1 illustrates the main body segments and key dimensions of the sailor. For this work the body is assumed to be symmetric.

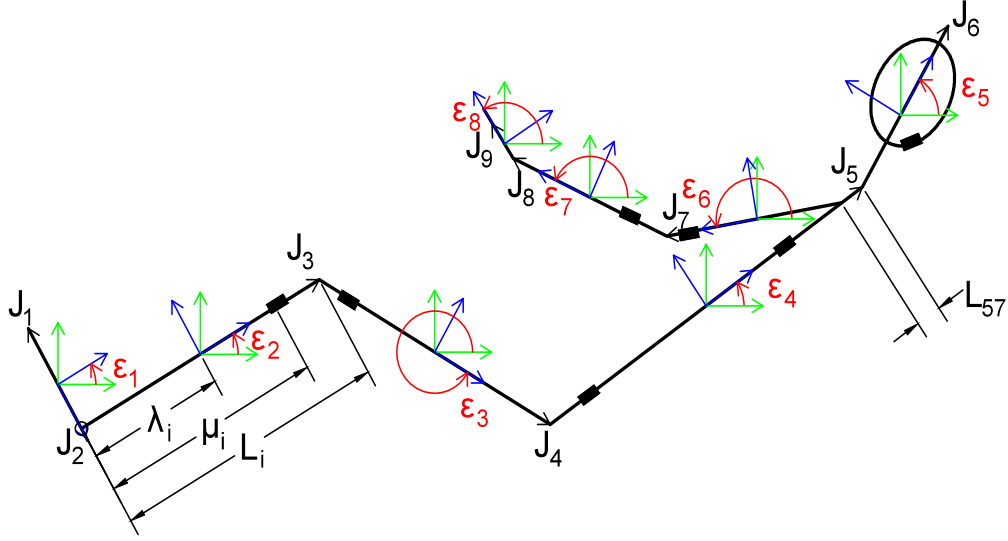


Figure 1 - Hiking Pose Schematic showing key dimensions and approximate sensor locations

The sailor's position is represented by a stick figure, as shown in Figure 1, where each line represents a body segment. The segments are linked using joints constrained at their endpoints in position but free to rotate. Each segment has a constant length, L_i^{seg} , measured for a given subject, as described in Figure 2, Table 1 and the vector set in equation (1).

$$L^{seg} = \begin{Bmatrix} L_1^{foot} \\ L_2^{shank} \\ L_3^{thigh} \\ L_4^{back} \\ L_5^{head \& neck} \\ L_6^{U-arm} \\ L_7^{L-arm} \\ L_8^{Hand} \end{Bmatrix} \quad (1)$$

static moment taken about a specific subject's ankles this equates to an error of only $\pm 0.6\%$ (0.4 Nm) for a 75 kg, 1.8 m tall individual. The curvature of the back is approximated as the interpolated orientation of the small of the back and the sternum using equation (3). For simplicity, only the left arm and leg are instrumented and limbs on the right side are assumed to mirror the left.

$$\epsilon^{seg} = \begin{Bmatrix} \epsilon_1^{foot} \\ \epsilon_2^{shank} \\ \epsilon_3^{thigh} \\ \epsilon_4^{back} \\ \epsilon_5^{head \& neck} \\ \epsilon_6^{U-arm} \\ \epsilon_7^{L-arm} \\ \epsilon_8^{Hand} \end{Bmatrix} \quad (2)$$

$$\epsilon_4^{back} = \frac{\epsilon_{41}^{L-back} + \epsilon_{42}^{sternum}}{2} \quad (3)$$

Table 1: Representative body segment details

Index	Segment	Origin	End Point	Length	Mass	COG	Rg x	Rg y	Rg z
1	Foot	HEEL	TTIP	258.1	1.4	44.2	25.7	24.5	12.4
2	Shank	KJC	LMAL	434.0	4.3	44.6	25.5	24.9	10.3
3	Thigh	HJC	KJC	422.2	14.2	41.0	32.9	32.9	14.9
4	Trunk	CERV	MIDH	603.3	43.5	51.4	32.8	30.6	16.9
5	Head	VERT	CERV	242.9	6.9	50.0	30.3	31.5	26.1
6	Upper arm	SJC	EJC	281.7	2.7	57.7	28.5	26.9	15.8
7	Forearm	EJC	WJC	268.9	1.6	45.7	27.6	26.5	12.1
8	Hand	WJC	MET3	86.2	0.6	79.0	62.8	51.3	40.1

The orientation and acceleration of each body segment is measured using Xsens' MTw inertial sensors (Xsens, 2013). These sensors provide an orientation expressed as a unit quaternion (a three dimensional rotation) dynamically stable to 2 degrees RMS. The highest impact of this error is when the subject is horizontal with their arms over their head and each body segment is rotated by 2 deg. For a

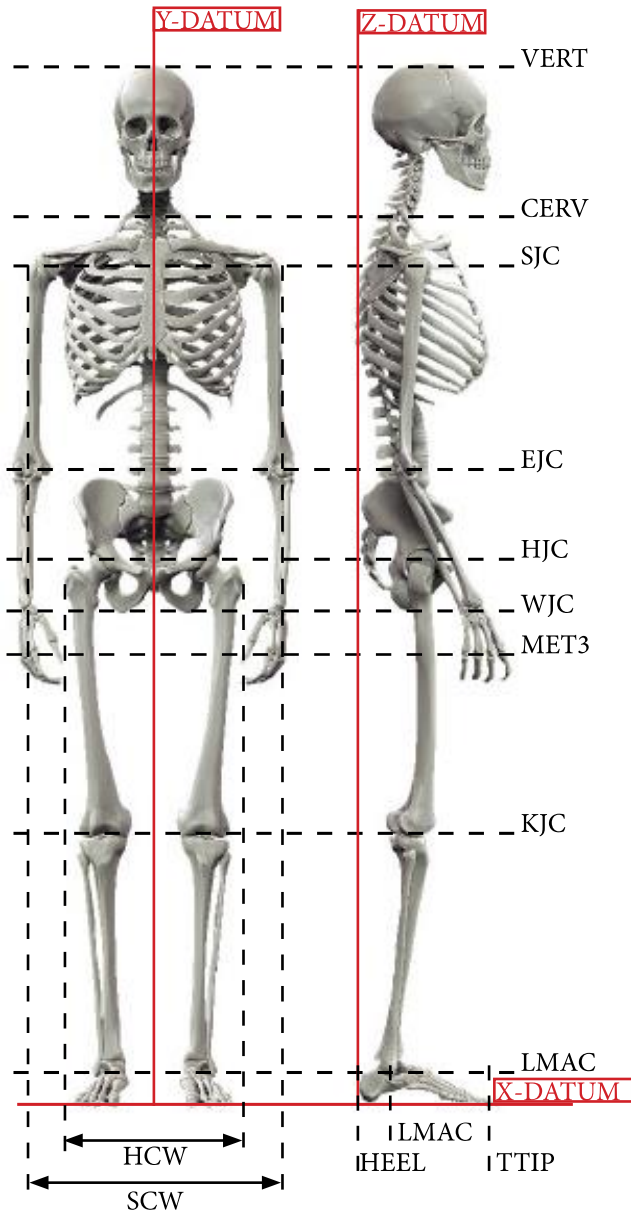


Figure 2 - Subject joint distances and anthropometric data

The mass and location of the centre of mass for each segment is required to convert the pose position into the generated force. There are several body-segment data sources in the literature. Models can be based on cadaver data which tend to have an elderly population. More recent studies use radiation to measure living subject's mass distribution. It is important for the studies' mean population to be close to the target population. There are two main methods for determining the mass distribution. The first assumes each body segment has uniform density. This relies on many measurements to define the geometry of each segment. The second method uses either proportional or regression based mass distribution methods using the subject height and mass (Zatsiorsky and

Seluyanov, 1983). A regression based mass model of Russian PE students is presented by Zatsiorsky (1983). This was later adjusted to reference more convenient segment boundaries located at joint centres and extended to include male and female data in a proportional mass model (Leva, 1996). For the purpose of this paper the later model will be used to define the mass distribution. An example of the resultant mass distribution for a 75kg, 1.8m tall male is presented in Table 1. The masses are given in kilograms, the centre of gravities (COG) are provided as a percentage of the segment lengths.

The following section uses quaternion rotations to switch frames of references. This provides a method which does not suffer from a mathematical singularity when pitch orientation approaches 90 degrees as Euler angles suffer from. The rotation notion used \mathbf{Q} to represent a quaternion and a superscript to represent the order of the rotation, where B represents the body segment, Y the yacht, G gravitational and S the sensor frame of reference. E.g. \mathbf{Q}_i^{BG} represents the quaternion to rotate from body to gravity frames of reference for segment i .

The orientation of the body segment to the gravity vector \mathbf{Q}^{BG} is calculated by finding the difference of the sensor orientation relative to gravity \mathbf{Q}^{SG} and the sensor to body orientation \mathbf{Q}^{SB} , as described in equation 4. \mathbf{Q}^{SB} is found by capturing a pose when the subject is lying down so the joint angles are zero.

$$\mathbf{Q}_i^{BG} = \mathbf{Q}_i^{SG} \times \text{inv}(\mathbf{Q}_i^{SB}) \quad (4)$$

A separate sensor mounted on the boat captures the yacht orientation and is zeroed when the boat is flat. This allows the orientation of the body segments relative to the yacht to be calculated.

A body segment is rotated to the sailor's pose using the body-yacht rotation \mathbf{Q}^{BY} , starting from the fixed point at the ankle. The body segment orientations therefore provide the coordinates for each joint, \mathbf{J}_i , moving up the body.

The linked chain pose is given by (5): -

$$\mathbf{J}_{i+1} = \left\{ \mathbf{Q}_i^{BY} \begin{bmatrix} L_i^{SG} \\ 0 \\ 0 \end{bmatrix} \right\} + \mathbf{J}_i \quad (5)$$

for $1 \leq i \leq 5$ and $7 \leq i$ where: -

$$\mathbf{Q}_i^{SB} = \mathbf{Q}_i^{SG} \text{ for zero pose}$$

The shoulder joint is not located at the end of the back segment therefore a non-dimensional distance is used to locate it between the neck and palpable point of the 5th vertebra.

The entire pose is then translated so the ankle joint, J_2 becomes the origin, as it will be used as the datum in experiments.

$$J = J - J_2 \quad (6)$$

Position vectors for segment centre of gravity, C_G and sensor positions S_{IMU} are defined for each segment in terms of COG coefficient, λ and sensor position coefficient, μ using equations (7) and (9) respectively. C_G is derived from published data (Zatsiorsky and Seluyanov, 1983; Leva, 1996; Dumas et al, 2007), given in table 1.

$$C_G = J_i + \lambda_i(J_i + J_{i+1}) \quad (7)$$

Where: -

$$\lambda_i = \frac{L_i^{COG}}{L_i^{seg}} \quad (8)$$

$$S_{IMU} = J_i + \mu(J_i + J_{i+1}) \quad (9)$$

Where: -

$$\mu_i = \frac{L_i^{IMU}}{L_i^{seg}} \quad (10)$$

For the on-water experiments the pose is offset by a measured vector found from the scaled video, providing the distance between the centreline of the dinghy at deck level, amidships and the midpoint between the sailor's ankles. The pose is finally rotated about the centreline of the dinghy to coincide with the roll angle (θ) of the boat:

$$C_{G_i}' = Q^{BG} C_G \quad (11)$$

The 3D acceleration, a' at C_{G_i}' is then used to calculate the generated hiking moment:

$$HM = CG_{xi}' m_{seg} a_z' \quad (12)$$

In summary, the following modelling assumptions have been made: -

- The head and neck are rigid and pivot about the palpable point of the 7th vertebrae.
- The back is straight and its curvature can be approximated by taking the mean of the upper and lower back orientations.

- The left limbs mirror the right limbs.
- The anthropometric model accurately predicts the segment COG.
- The mass distribution (i.e. the relative mass of each segment) can be adjusted to tune the model for a given subject if required.

ESTIMATED POSE LOAD VALIDATION



Figure 3 - Schematic of direct measurement of hiking moment

The pose algorithm is validated using a board with one end resting on a set of scales, as depicted in Figure 3. As the total mass of the subject and the length of the board is known the position of the centre of gravity, and hence the hiking moment about the ankles, can be calculated. The subject is asked to hold a set of poses chosen to isolate the effect each body segment has on hiking moment. Each of these poses are held for 30 seconds.

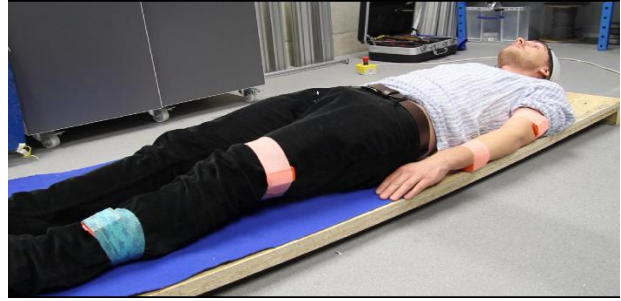
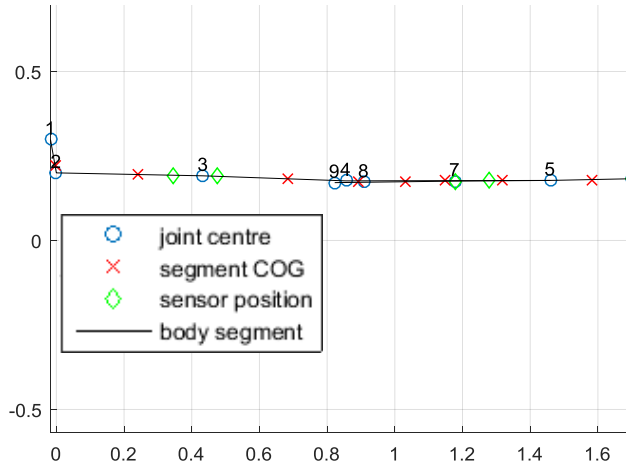


Figure 4 - Direct measurement of Hiking Moment to validate Pose capture system.

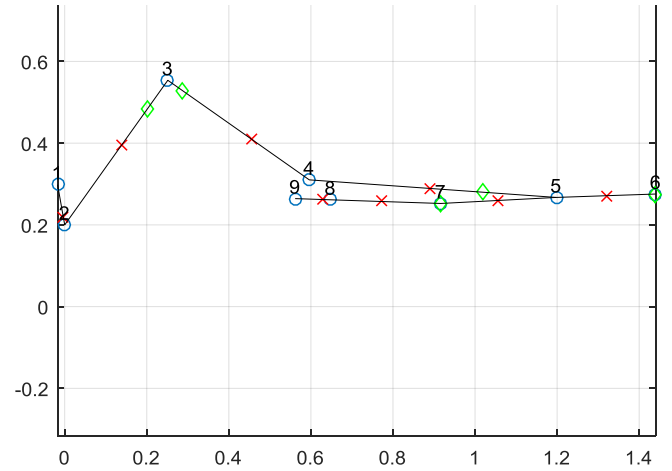
Each segment's centre of gravity given by Leva (1996) is assumed to be correct and the mass is redistributed from the initial assumed values using equation (13). The estimated mass of the feet is assumed correct (relative mass 2.8% m_{aser}) since the feet location is close to the centreline.

$$m_i^{cal} = m_i^{seg} \left(\frac{m_{slr}}{\sum m_i^{seg}} \right) \quad (13)$$

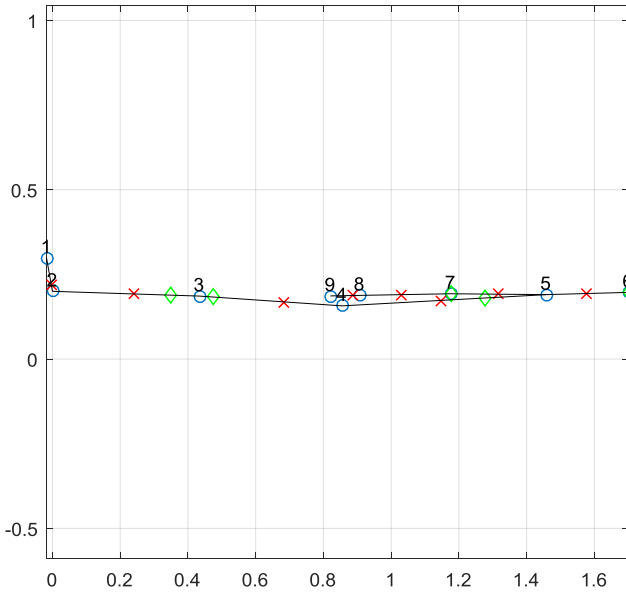
VALIDATION RESULTS



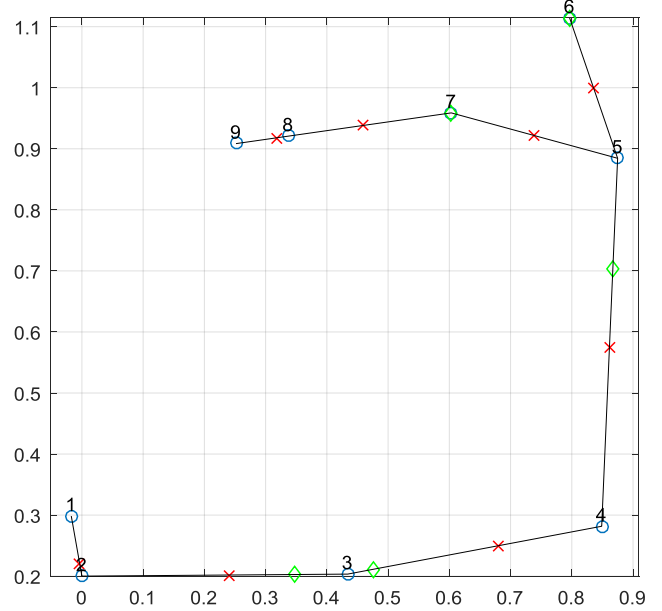
(a) Pose 1



(b) Pose 3



(c) Pose 5 (Repeat of Pose 1)



(d) Pose 10

Figure 5 Four examples of the pose captured by the inertial sensor system using the flat board. Axes are in m relative to ankle joint

A series of 13 body positions were conducted during the pose validation process. The comparison between the direct measurement of the hiking moment and the estimate provided by the pose capture system is provided in Table 2. A number of the captured poses are provided in Figure 5 for visual reference.

The baseline position depicted in Figure 4 was conducted several times to check the repeatability of the system. It can be seen in Table 4 that, although the hiking moment calculated from the pose capture system repeatedly estimated the same value, the measured value from the board and scales varies slightly. This is most likely due to a slight change in the position of the ankle (i.e. a longitudinal change in the position of the subject on

the measurement board). Comparing pose 5 with pose 1, in Figure 5, it is evident that either the physical sensor position has moved or the sensors are drifting as there are slight changes in the captured pose for the repeated position. Many factors could be contributing to this, including the movement and stretching of clothing, the presence of high voltage/current electrical cables present in the test venue or slightly different physical positions being adopted by the subject.

Table 2 – Comparison of measured Hiking Moment (HM) compared to the estimate from the pose capture system. (Poses 2-4 did not maintain the ankle at the end of the board, therefore had to have the measured HM corrected for comparison)

Pose#	HM Measured (Nm)	HM from Pose (Nm)	Error
1	713	707	-1%
2	57	54	-5%
3	525	534	2%
4	513	547	7%
5	710	707	0%
6	574	551	-4%
7	567	543	-4%
8	551	531	-4%
9	563	533	-5%
10	539	531	-1%
11	547	537	-2%
12	562	535	-5%
13	692	707	2%

On average the pose capture system was observed to correctly estimate the hiking moment generated in a range of different positions within 5% accuracy. Therefore, it was concluded that the system would provide useful measurements of the on water hiking position of sailors. However, it must be accepted that this as yet does not represent a detailed study of the sailing population. The results relate to a single subject and neglect dynamic loads. The validation procedure should be extended to account for this by imposing motion and comparing pose data with load cell data on an instrumented platform.

ON THE WATER METHODOLOGY

To establish if the developed pose-capture methodology would work out on the water an initial case study was conducted using a Laser Radial sailing dinghy. The Laser is a small solo planing dinghy class. The craft is LWL = 3.81m, BWL = 1.37m Δ > 58.9kg. SA = 7.06m² (Laser, 2012).

To enable the boat motions to be captured the same model Xsens IMU was attached to the right of the dagger-board's leading edge. A 10Hz GPS receiver is used to track the boat's speed and course over ground. The inertial

sensors used to capture the athlete's pose wirelessly stream the data to a tablet that logs the data. The estimated combined weight of the instrumentation was approaching 10kg. All of this mass was carried forward of the mast which significantly affected boat motions and acts as a weight penalty. The equipment can be observed in Figure 6.



Figure 6 – On water equipment

The experiments were conducted close to slack water to minimise tidal effects. The ankles are taken as the pose datum so the mounted video can be used to measure their offset away from the centreline in post-processing using video footage captured from a tiller-mounted camera, as shown in Figure 7. The sensor positions on both the sailor and boat are chosen for the best compromise between being close to the segment centre of gravity and located on a rigid part of the body (i.e. close to the bone) to reduce skin movement artefacts.

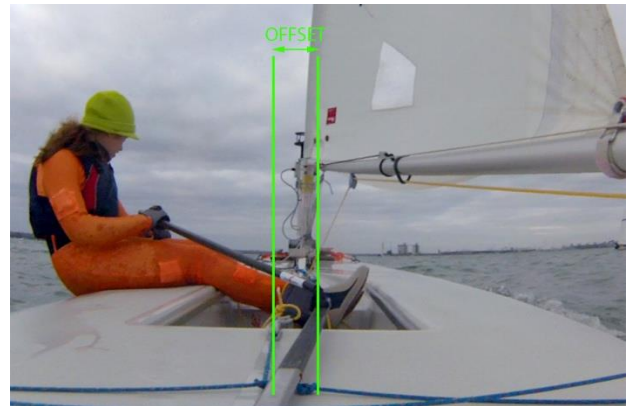


Figure 7 Using video to offset pose

The GPS track of the on-water data recording session is provided in Figure 8. A representative plot of the unsteady Hiking moment acquired by the pose capture system is provided in Figure 9. This initial on the water study shows that the developed system can work in a real sailing situation enabling valuable dynamic hiking moment data to be obtained. The presented data is from a lit wind condition where the boats roll angle can be seen to respond to changes in generated hiking moment.

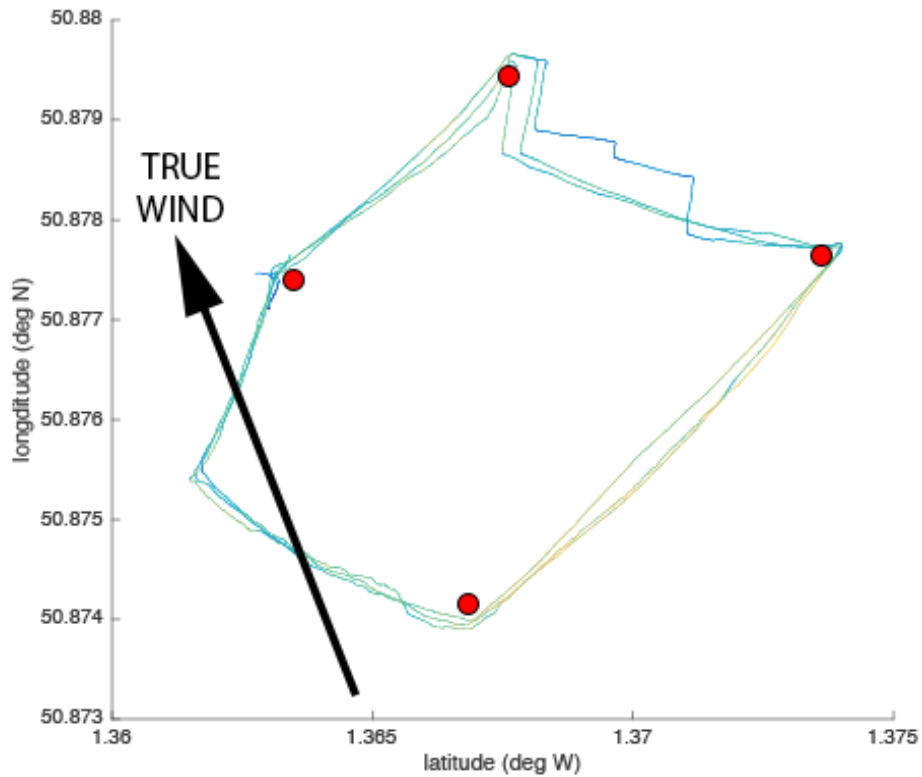


Figure 8 GPS track of Race, with line colour representing boat speed.

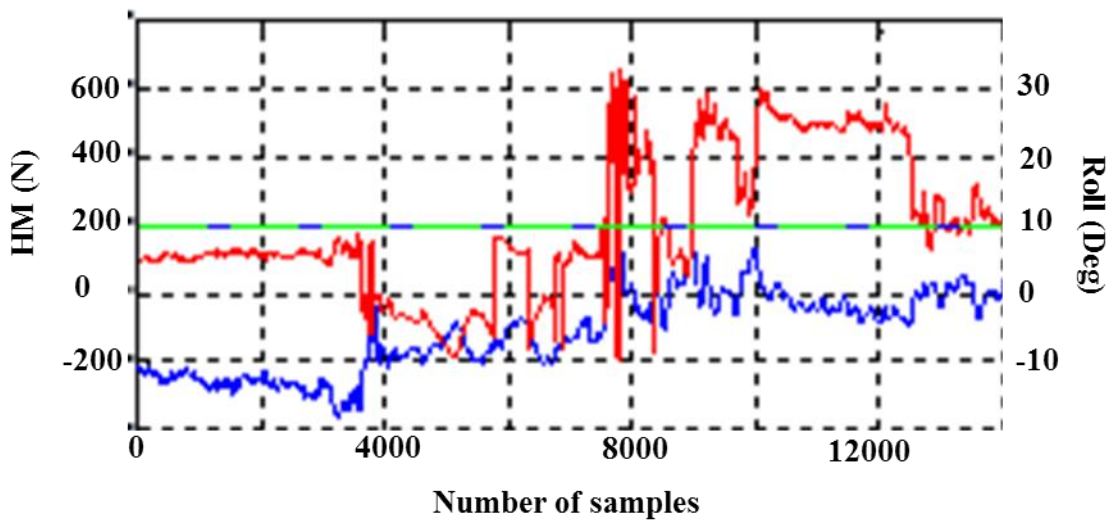


Figure 9 Light wind example of measured Unsteady Hiking Moment (Red) compared to roll angle (Blue) from on the water tests.

FUTURE APPLICATION TO A DYNAMIC VPP

The ability to acquire unsteady hiking moments relative to boat motions allows these loadings to be characterised and fed back into a fully dynamic VPP algorithm in the future. This could be coupled with unsteady wind, sail and

foil models to provide a more realistic evaluation tool for sailing dinghy performance. The next stage in the work is to classify the sailor position and adjustment during typical race phases. From these a model can be developed to use within the dynamic VPP.

The single-handed sailor is the human-in-the-loop controller for the selection of the 'best' performance of the yacht through adjustment of position, helm angle and trim of sails. Previous work (Spenkuch, 2014; 2011, 2010) demonstrates that understanding the tactical and strategic behaviour of competitor sailors requires the unsteady physics of the yacht performance to be captured realistically enough.

CONCLUSION

The work has demonstrated that a network of appropriately located inertial motions sensors can provide assessment of both pose and motion. The ability to estimate the developed hiking moment provides an opportunity to better understand the on-water performance of dinghies in the stochastic environmental challenge of wind and waves.

The developed system still requires some further development to reduce its mass and on-board footprint. One area requiring further work is in ensuring automated operation with minimal interaction required of the sailor.

The development work has used a limited set of sailors and in the next phase a wider group will be studied for pose and motion calibration within a laboratory environment. On-water studies will move onto the International Moth once remaining mass issues are resolved.

ACKNOWLEDGEMENTS

The author's gratefully acknowledge the funding support of the EPSRC iCASE Studentship which support Josh Taylor's PhD from the English Institute of Sport (Research and Innovation). All work requiring ethical approval has been registered through the Faculty of Engineering and Environment ethics review process.

REFERENCES

- L.-M. Breschan, A. Lidtke, L. M. Giovannetti, A. Sampson, and M. Vitti, "America's Cup Catamaran Tacking Simulator," Southampton University Group Design Project Thesis for MEng Ship Science degree course, 2013.
- S.S. Bennett, C.J. Brooks, B. Winden, D.J. Taunton, A.I.J. Forrester, S.R. Turnock, D.A. Hudson, "Measurement of ship hydroelastic response using multiple wireless sensor nodes", *Ocean Eng.*, Vol. 79, 67–80. 2014.
- R. Dumas, L. Chèze, and J.-P. Verriest, "Adjustments to McConville et al. and Young et al. body segment inertial parameters," *J. Biomech.*, vol. 40, no. 3, pp. 543–553, Jan. 2007.
- E. J. De Ridder, K. J. Vermeulen, and J. A. Keuning, "A Mathematical Model for the Tacking Maneuver of a Sailing Yacht," *Int. HISWA Symp. Yacht Des. Yacht Constr.*, pp. 1–34, 2004.

- M. W. Findlay and S. R. Turnock, "Development and use of a Velocity Prediction Program to compare the effects of changes to foil arrangement on a hydro-foiling Moth dinghy," *Proceedings Int. Conf. Innov. High Perform. Sail. Yachts.*, 2008.
- ISAF, *INTERPRETATIONS OF RULE 42, PROPULSION*, May. 2013.
- J. Keuning and E. De Ridder, "A Generic Mathematical Model for the Maneuvering and Tacking of a Sailing Yacht," *Chesap. Sail. Yacht Symp.*, no. 1458, pp. 143–163, 2005.
- Laser Class Association, "Laser Class Rules," 2012.
- P. de Leva, "Adjustments to Zatsiorsky-Seluyanov's segment inertia parameters," *J. Biomech.*, vol. 29, no. 9, pp. 1223–1230, Sep. 1996.
- Y. Masayuma, T. Fukasawa, and H. Sasagawa, "Tacking Simulation of Sailing Yachts – Numerical Integration of Equations of Motion and Application of Neural Network Technique," *12th Chesap. Sail. Yacht Symp.*, 1995.
- C. Phillips, A. Forrester, D. Hudson, S. Turnock, "Comparison of Kinematic Acquisition Methods for Musculoskeletal Analysis of Underwater Flykick", *Procedia Eng.*, Vol 72, 2014, 56–61.
- T. Spenkuch, S. Turnock, M. Scarponi, and A. Sheno, "Real time simulation of tacking yachts: how best to counter the advantage of an upwind yacht," *Procedia Eng.*, vol. 2, no. 2, pp. 3305–3310, Jun. 2010.
- T. B. Spenkuch, "UNIVERSITY OF SOUTHAMPTON A Bayesian Belief Network Approach for Modelling Tactical Decision-Making in a Multiple Yacht Race Simulator By," no. April, 2014.
- T. Spenkuch, S. R. Turnock, M. Scarponi, and R. A. Sheno, "Modelling multiple yacht sailing interactions between upwind sailing yachts," *J. Mar. Sci. Technol.*, vol. 16, pp. 115–128, 2011.
- T. Spenkuch, S. Turnock, M. Scarponi, and A. Sheno, "Real time simulation of tacking yachts: How best to counter the advantage of an upwind yacht," *Procedia Eng.*, vol. 2, no. 2, pp. 3305–3310, 2010.
- Xsens, "MTw User Manual", Document MW0502P, Revision H, 2013. (https://www.xsens.com/download/usermanual/MTw_usermanual.pdf)
- Zatsiorsky and Seluyanov, "The mass and inertia characteristics of the main segments of the human body," *Biomechanics*, 1983.

AUTHORS BIOGRAPHY

Josh Taylor is a BEng graduate of the University of Newcastle-upon-Tyne. He is a keen sailor and is now pursuing his Doctoral studies in the Performance Sports Engineering Lab at the University of Southampton.

Dr Joe Banks is a New Frontiers Fellow at the University

of Southampton where he also completed his Master of Engineering and PhD. In this he worked closely with UKSport (now EIS) Research and Innovation in the run upto London 2012. His current research focusses on the development of experimental techniques to capture time accurate coupled fluid structure interaction alongside Computational Fluid Dynamics.

Professor Stephen Turnock directs the Performance Sports Engineering Lab at the University of Southampton. He is a graduate of Cambridge(MA), MIT (SM) and Southampton (PhD). He leads the Maritime Engineering group in the Faculty of Engineering and Environment and in recent years has led the fitout of the new wave/towing tank (138m x 6m x 3.5m, max speed 12m/s). His research interests ship hydrodynamics, renewable energy, autonomy alongside his interests in performance sport.